A Molecular Model for Solid-State Polymerization of Nylon 6

A. KAUSHIK and S. K. GUPTA*

Department of Chemical Engineering, Indian Institute of Technology, Kanpur 208 016, India

SYNOPSIS

A theoretical model is developed for the effect of segmental diffusion on reversible step growth polymerization. This model is an adaptation of the molecular model of Chiu et al. for characterizing the Trommsdorff effect in free-radical polymerization. The model is applied to the specific case of solid-state polymerization of spherical pellets of nylon 6. The results of the simulation are found to show qualitative trends as found by Gaymans et al. experimentally. The parameters of the model are curve fitted to their data using an optimal parameter estimation computer code. It is found that the optimal values of the parameters, which can be independently measured, are quite close to the values reported in the literature. The effect of varying the individual parameters on the progress of polymerization is also studied.

INTRODUCTION

Several condensation polymers like polyacrylamides, polyesters, and polyamides are known to polymerize at temperatures between their melting and glass transition points. This phenomenon is commonly known as solid-state polymerization (SSP). SSP can take place both with crystalline monomers[1] as well as with semicrystalline prepolymers. In the latter case this phenomenon is also known as postcondensation.

SSP is a subject of special interest in the field of polymers. The SSP of crystalline monomers has so far been confined to laboratories and is generally not employed for commercial purposes. On the other hand, SSP of semicrystalline prepolymers has received widespread attention in industry. This is mainly because the postcondensation of prepolymers leads to polymers of very high chain lengths, usually not obtainable in the molten state (due to limitations posed by equilibrium, etc.), and one obtains materials having improved mechanical and thermal properties. Usually, medium to low molecular weight semicrystalline prepolymers, in the form of small chips, are subjected to further polymerization at temperatures between the melting point and the glass transition temperature of the polymer. Condensation by-products are removed by carrying out the process in a stream of inert gas or in vacuum to facilitate increase in chain length. An excellent literature review of SSP has recently been reported by Pilati.[1]

A comprehensive effort to understand the postcondensation process started over three decades ago. Several experimental studies were reported in the literature. Attempts on the interpretation of experimental data, however, were quite dispersed. A few workers also tried to develop mathematical models to explain the data. Notable among these is the study of Chen et al.[2] Unfortunately, models proposed are semiempirical in nature and often have little molecular basis. Because of this design of industrial postcondensation reactors is still an art.

Recently, Chiu et al.[3] have presented a phenomenological model having a sound molecular basis, for predicting the effect of segmental diffusion on the termination rate constant of free-radical polymerizations. Kumar et al.[4] adapted this model for irreversible step growth polymerizations and presented simulation results for the increase in chain length with time, in the presence of segmental diffusional resistances. The present study is an exten-

* To whom correspondence should be addressed.

Journal of Applied Polymer Science, Vol. 45, 507–520 (1992)
 CCC 0021-8995/92/030507-14$04.00

sion of the latter work. A mathematical model accounting for the low rates of segmental diffusion on *reversible* step growth polymerizations of ARB prepolymers is developed. This model is then used to simulate the solid-state polymerization of nylon 6. An optimal parameter estimation software package is used to obtain the best-fit values of the parameters used in the model, using experimental data of Gaymans et al.[5]

Any attempt at mathematical modeling of the phenomenon of postcondensation should consider the three possible rate-determining steps:

1. Chemical reaction (inclusive of the "micro level" diffusion of polymer molecules).
2. Diffusion (macro level) of the condensation by-products from the inside of the reacting mass/pellet to the surface. This is important for reversible reactions.
3. Diffusion of the by-product molecules from the solid polymer surface to the surrounding inert gas.

Griskey and Lee[6] and Gaymans et al.[5] have concluded on the basis of their experiments that step 1 is the rate-controlling step, and the diffusion of by-products both within the pellet and from the surface of the pellet to the inert gas do not affect the progress of reaction. The same conclusion is drawn in the theoretical analysis of Chen et al.[2] The present study, however, incorporates the effect of (micro) diffusion of reactive end groups as well as the diffusion of the condensation by-products. The study attempts to explain the available experimental data on the influence of the starting molecular weight on the progress of the reaction, as well as the effect of remelting (homogenizing) the polymer sample in between the polymerization. The study presented, thus, attempts to explain, on the basis of a molecular model, the conclusions drawn by Gaymans et al.[5] in their experimental study and so establishes a basis for a more rational design of postcondensation industrial reactors in the future.

FORMULATION

The kinetic scheme for nylon 6 polymerization is shown in Table I. The three major reversible reactions—ring opening, polycondensation, and polyaddition—are shown. The rate constants, k_{li} and k'_{li}, associated with these reactions *in the liquid phase,* are given in Table II, while the appropriate mass-balance equations for a well-mixed batch reactor (reaction in liquid phase) are shown in Table III. These are well documented[7,8] and have been found to be quite satisfactory for the simulation of industrial nylon 6 reactors.

Table I Kinetic Scheme for Polymerization of Nylon 6 in Liquid Phase

1. $C_1 + W \underset{k'_{l1}}{\overset{k_{l1}}{\rightleftarrows}} P_1$ (ring opening)
2. $P_n + P_m \underset{k'_{l2}}{\overset{k_{l2}}{\rightleftarrows}} P_{n+m} + W$ (polycondensation)
3. $P_n + C_1 \underset{k'_{l3}}{\overset{k_{l3}}{\rightleftarrows}} P_{n+1}$ (polyaddition)

From Table I it is observed that the reaction that is most susceptible to (micro) diffusional limitations is the forward step in the polycondensation reaction:

$$P_n + P_m \underset{k'_p}{\overset{k_p}{\rightleftarrows}} P_{m+n} + W \tag{1}$$

since two macromolecules have to come together for reaction, it is this reaction that will be affected by diffusional effects when the polymerization is carried out in the solid phase. This is why we have used new rate constants, k_p and k'_p, in Eq. (1). We now attempt to develop a model for k_p along the lines of Chiu et al.[3] and Kumar et al.[4]

One focuses attention on a polymer chain, P_n, with its A functional group located at the center of a sphere of radius r_m (see Fig. 1). The reaction between this functional group and a B group of another molecule, P_m, occurs after the latter comes in the vicinity of A by segmental diffusion as well as by reaction due to the other possibilities shown in Table I. The spatial variation of functional group B is identical to the spatial variation of the concentration, $[P]$ ($=[\text{---A}] = [\text{---B}] = \sum_{n=1}^{\infty} [P_n]$), of polymer P, because there is one unreacted B group per chain for ARB polymerizations.

Assuming that the concentration of polymer P at a "large" distance, r_D, from the central functional group A, approaches the (local) bulk value, $[P]_b$, and that the effective concentration at r_m is $[P]_m$, one has at steady state (see Refs. 3 and 4 for complete details)

$$4\pi r^2 D \frac{d[P]}{dr} = C \tag{2}$$

Table II Rate and Equilibrium Constants for Liquid Phase Reaction

i	A_i^0 (kg/mol h)	E_i^0 (J/mol)	A_i^c (kg^2/mol^2 h)	E_i^c (J/mol)	ΔH_i (J/mol K)	ΔS_i (J/mol K)
1	5.9874×10^5	8.3170×10^4	4.3075×10^7	7.8864×10^4	8.0249×10^3	-3.2989×10^1
2	1.8942×10^{10}	9.7365×10^4	1.2114×10^{10}	8.6483×10^4	-2.4877×10^4	3.9846
3	2.8558×10^9	9.5583×10^4	1.6377×10^{10}	8.4127×10^4	-1.6919×10^4	-2.906×10^1

$$k_{li} = A_i^0 \exp(-E_i^0/RT) + A_i^c \exp(-E_i^c/RT) \sum_{n=1}^{\infty} [P_n]$$

$$= k_{li}^0 + k_{li}^c \sum_{n=1}^{\infty} [P_n]$$

$$K_i = \exp[(\Delta S_i - \Delta H_i/T)/R]$$

$$k'_{li} = \frac{k_{li}}{K_i} \qquad i = 1, 2, 3$$

with boundary conditions

$$\text{at} \quad r = r_m \qquad [P] = [P]_m \qquad (3a)$$

$$\text{at} \quad r = r_D \to \infty \qquad [P] = [P]_b \qquad (3b)$$

where, as before,

$$[P] = \sum_{n=1}^{\infty} [P_n] \qquad (4)$$

In Eq. (2) D is the overall diffusivity of the polymer molecules and C is a constant equal to the rate of consumption of functional group B at $r = r_m$, by reaction. Integration of Eq. (2) with $r_D \to \infty$ yields (as in Refs. 3 and 4),

$$4\pi D r_m([P]_b - [P]_m) = C \qquad (5)$$

For the reversible step growth reaction shown in Eq. (1), the rate of consumption of B, by reaction within the sphere of radius r_m, can be written as

$$C = (\tfrac{4}{3})\pi r_m^3 \{k_{p0}[P]_m[P]_b - k'_{p0}[W][\text{—AB—}]_b\} \qquad (6)$$

Table III Mole Balance Equations for Polymerization of Nylon 6 in Liquid Phase[a]

1. $\dfrac{dC_1}{dt} = -k_{l1}C_1W + k'_{l1}P_1 - k_{l3}C_1\lambda_0 + k'_{l3}(\lambda_0 - P_1)$
2. $\dfrac{dP_1}{dt} = k_{l1}C_1W - k'_{l1}P_1 - 2k_{l2}P_1\lambda_0 + 2k'_{l2}W(\lambda_0 - P_1) - k_{l3}P_1C_1 + k'_{l3}P_2$
3. $\dfrac{d\lambda_0}{dt} = k_{l1}C_1W - k'_{l1}P_1 - k_{l2}\lambda_0^2 + k'_{l2}(\lambda_1 - \lambda_0)W$
4. $\dfrac{d\lambda_1}{dt} = k_{l1}C_1W - k'_{l1}P_1 + k_{l3}C_1\lambda_0 - k'_{l3}(\lambda_0 - P_1)$
5. $\dfrac{d\lambda_2}{dt} = k_{l1}C_1W - k'_{l1}P_1 + 2k_{l2}\lambda_1^2 + \frac{1}{3}k'_{l2}W(\lambda_1 - \lambda_3) + k_{l3}C_1(\lambda_0 + 2\lambda_1) + k'_{l3}(\lambda_0 - 2\lambda_1 + P_1)$
6. $\dfrac{dW}{dt} = -k_{l1}C_1W + k'_{l1}P_1 + k_{l2}\lambda_0^2 - k'_{l2}(\lambda_1 - \lambda_0)W$

Closure conditions

7. $P_2 = P_1$
8. $\lambda_3 = \lambda_2(2\lambda_2\lambda_0 - \lambda_1^2)/(\lambda_1\lambda_0)$

where $\lambda_k = \sum_{n=1}^{\infty} n^k[P_n]$

[a] Brackets, [ ], for concentrations omitted for brevity.

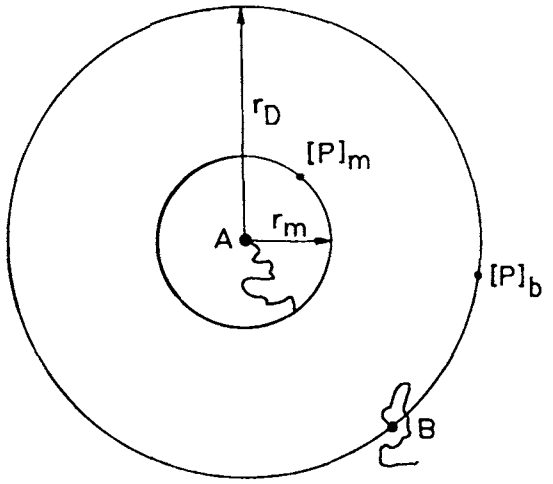

Figure 1 Segmental diffusion of a polymer molecule with an unreacted B group toward another polymer molecule with an unreacted A group.

where the subscripts 0 on k_p and k'_p indicate that the intrinsic rate constants are being used. It is assumed that no diffusional resistances exist for W since it is a small molecule. Using

$$[\text{—AB—}]_b = [\lambda_1 - \lambda_0]_b = [\lambda_{1b} - [P]_b] \quad (7)$$

we obtain

$$C = (\tfrac{4}{3})\pi r_m^3 \{k_{p0}[P]_m[P]_b - k'_{p0}[W][\lambda_{1b} - [P]_b]\} \quad (8)$$

Equations (5) and (8) yield $[P]_m$ as

$$[P]_m = \frac{[P]_b\{D - (r_m^2/3)k'_{p0}[W]\} + k'_{p0}\lambda_{1b}(r_m^2/3)}{D + (r_m^2/3)k_{p0}[P]_b} \quad (9)$$

The overall polymerization rate (i.e., for P) for the reversible reaction shown in Eq. (1) can be written as $k_p[P]_b^2 - k'_p[W]\{\lambda_{1b} - [P]_b\}$. Equating this to the rate given in Eq. (8) leads to

$$\{k_p[P]_b^2 - k'_p[W][\lambda_{1b} - [P]_b]\} = \{k_{p0}[P]_m[P]_b - k'_{p0}[W][\lambda_{1b} - [P]_b]\} \quad (10)$$

Assuming that the diffusional effects are significant only for the forward reaction and negligible for the reverse reaction,

$$k'_p = k'_{p0} \quad (11)$$

One obtains from Eq. (10)

$$k_p[P]_b^2 = k_{p0}[P]_m[P]_b \quad (12)$$

or,

$$[P]_m = \left(\frac{k_p}{k_{p0}}\right)[P]_b \quad (13)$$

Equations (9) and (13) give on comparison and rearrangement,

$$\frac{k_p}{k_{p0}} = \frac{1 - (r_m^2/3D)k'_p[W]\{1 - (\lambda_1/\lambda_0)\}}{1 + (r_m^2/3D)k_{p0}\lambda_0} \quad (14)$$

where the subscripts, b, on the λ's have been dropped.

Equation (14) gives the final relationship between the overall rate constant of reaction, k_p (in the presence of diffusional limitations) and the intrinsic rate constant of reaction, k_{p0}. We find that the ratio, k_p/k_{p0}, is a function of the diffusivity of the polymer molecule, D, the distance of diffusion, r_m, the concentration of water, $[W]$, and of polymer, λ_0, and the first moment, λ_1. It is also a function of the reverse rate constant, k'_p.

The term $r_m^2/3D$ in Eq. (14) incorporates the diffusional distance and diffusivity of polymer molecules. It has the units of time and can be written in analogy with Chiu et al.[3] as

$$\frac{r_m^2}{3D} = \frac{(r_m^2/3D_0)}{D/D_0} \equiv \frac{\theta_t}{D/D_0} \quad (15)$$

where D_0 is the diffusivity at some reference state and θ_t can be considered as a parameter in this model, much like what was done for polymethylmethacrylate.[3]

The dependence of D/D_0 on the reaction temperature and polymer concentration is assumed to be given[3,4,9] by the Fujita–Doolittle theory:

$$\frac{D}{D_0} = \exp\left[\frac{(2.303v_f)}{\{A(T) + B(T)v_f\}}\right] \quad (16)$$

where v_f is the free volume fraction, and $A(T)$ and $B(T)$ are empirically determined functions of temperature. For isothermal conditions they are constants. Again $A(T)$ and $B(T)$ can be used as parameters in this model.

The free volume fraction[4,9] for step growth polymerization reaction systems can be given by

$$v_f = 0.025 + (\alpha_l - \alpha_g)(T - T_g) \qquad (17)$$

where α_l and α_g are the volume expansion coefficients of the liquid and the glassy polymer, T is the reaction temperature, and T_g is the glass transition temperature of the reaction mass. T_g is a function of the chain length and increases as the chain length of the polymer increases. The following equation is used to evaluate the glass transition temperature, T_g,

$$\frac{1}{T_g} = \frac{1}{T_{g\infty}} + \frac{K_s}{T_{g\infty}^2}\frac{1}{\bar{\mu}_n} \qquad (18)$$

where μ_n is the number-average chain length and K_s and $T_{g\infty}$ are empirical constants. We have used the spatially averaged (over the entire particle) value of μ_n to evaluate T_g to keep the analysis simple. It is found that this assumption does not have any significant effect on the results.

Solid-state polymerization is carried out in practice using pellets in a stream of flowing gas (or under vacuum) to facilitate the removal of the by-product, W, from the reacting pellets. We consider the reacting pellets to be spherical. The condensation by-product, W, diffuses out radially through the spherical pellet. It is assumed that the (macroscopic) diffusivity of water, D_w, in the pellet is constant. For a spherical pellet with diffusion in the radial direction only, one can write the mass balance equation as

$$\frac{\partial[W]}{\partial t} = D_w \frac{1}{r^2}\frac{\partial}{\partial r}\left(r^2 \frac{\partial[W]}{\partial r}\right) + R_w \qquad (19)$$

where R_w is the rate of "generation" of water by chemical reaction [Eq. (1)], given by

$$R_w = k_p\lambda_0^2 - k_p'[W](\lambda_1 - \lambda_0) \qquad (20)$$

Hence,

$$\frac{\partial[W]}{\partial t} = D_w\left(\frac{\partial^2[W]}{\partial r^2} + \frac{2}{r}\frac{\partial[W]}{\partial r}\right) + k_p\lambda_0^2 - k_p'[W](\lambda_1 - \lambda_0) \qquad (21)$$

The initial condition can be taken as a uniform distribution of W in the pellet,

$$t = 0 \qquad [W] = [W]_0 \qquad (22)$$

and the boundary conditions are

$$r = 0 \qquad \frac{\partial[W]}{\partial r} = 0 \qquad (23a)$$

$$r = R \qquad [W] = [W]_s \qquad (23b)$$

The surface concentration, $[W]_s$, depends on the vacuum applied. Vapor–solid equilibrium concepts can be applied to determine $[W]_s$ as a function of time, but this is not done here to keep the computations simple, and $[W]_s$ is taken as a constant.

In order to solve these equations, one needs equations for λ_1 and λ_0. These can easily be obtained using the complete kinetic scheme for nylon 6 polymerization in the solid phase. Table IV shows the scheme used. The subscript s on the rate constants indicates the values corresponding to the solid-state polymerization. It is observed that Table IV incorporates the polycondensation and polyaddition reactions only. The first reaction in Table I has been omitted to keep the analysis simple (in fact, it is expected that chain growth will occur primarily by the polycondensation reaction of Table I and even the polyaddition reaction will not contribute much). The mole balance equations for solid-state polymerization are listed in Table V. The finite-difference technique in the r direction has been applied to reduce the partial differential equation [Eq. (21)] to a set of coupled ordinary differential equations. These equations for $[W]$, along with the equations of the other species (Table V), are solved numerically using the subroutine D02EBF from a NAG FORTRAN library. The subroutine is based on Gear's method for solving a set of coupled, nonlinear, ordinary differential equations.

In order to obtain the initial values of the concentration of ϵ-caprolactam, C_1, amino caproic acid, P_1, and water, W, and the zeroth, first, and second moments, λ_0, λ_1, and λ_2, respectively, for simulating polymerization in the solid phase, we first simulated the isothermal liquid phase polymerization (integrated the equations in Table III) with $[W]_0 = 0.16$ mol/kg, $[C_1]_0 = 8.8$ mol/kg, and $T = 513.0$ K, until a desired value of the number-average chain length,

Table IV Kinetic Scheme for Polymerization of Nylon 6 in Solid Phase

$P_n + P_m \underset{k'_{s2}}{\overset{k_{s2}}{\rightleftarrows}} P_{n+m} + W$	(diffusion controlled polycondensation)
$P_n + C_1 \underset{k'_{s3}}{\overset{k_{s3}}{\rightleftarrows}} P_{n+1}$	(polyaddition)

Table V Final Equations for Polymerization of Nylon 6 in Solid Phase[a]

A. Balance Equations

1. $\dfrac{\partial C_1}{\partial t} = -k_{s3}C_1\lambda_0 + k'_{s3}(\lambda_0 - P_1)$

2. $\dfrac{\partial P_1}{\partial t} = -2k_{s2}P_1\lambda_0 + 2k'_{s2}W(\lambda_0 - P_1) - k_{s3}P_1C_1 + k'_{s3}P_2$

3. $\dfrac{\partial \lambda_0}{\partial t} = -k_{s2}\lambda_0^2 + k'_{s2}W(\lambda_1 - \lambda_0)$

4. $\dfrac{\partial \lambda_1}{\partial t} = k_{s3}C_1\lambda_0 - k'_{s3}(\lambda_0 - P_1)$

5. $\dfrac{\partial \lambda_2}{\partial t} = 2k_{s2}\lambda_1^2 + \frac{1}{3}k'_{s2}W(\lambda_1 - \lambda_3) + k_{s3}C_1(\lambda_0 + 2\lambda_1) + k'_{s3}(\lambda_0 - 2\lambda_1 + P_1)$

6. $\dfrac{\partial W}{\partial t} = k_{s2}\lambda_0^2 - k'_{s2}W(\lambda_1 - \lambda_0) + D_w\left(\dfrac{\partial^2 W}{\partial r^2} + \dfrac{2}{r}\dfrac{\partial W}{\partial r}\right)$

Initial conditions

7a. at $t = 0$ values from Table VI

Boundary conditions

7b. at $r = 0$ $\dfrac{\partial W}{\partial r} = 0$

7c. at $r = R$ $W = W_s$

Closure conditions

8. $P_2 = P_1$

9. $\lambda_3 = \lambda_2(2\lambda_2\lambda_0 - \lambda_1^2)/(\lambda_1\lambda_0)$

B. Equations for Rate Constants

10. $k_{s2,0} = \zeta_2(T)\lambda_0$

11. $k_{s3} = k_{s3,0} = \zeta_3(T)\lambda_0$

12. $k'_{s2} = k'_{s2,0} = k_{s2,0}/K_2$

13. $k'_{s3} = k'_{s3,0} = k_{s3,0}/K_3$

14. $k_{s2} = k_{s2,0}\left[\dfrac{1 - \{\theta_t/(D/D_0)\}k'_{s2}W(1 - \lambda_1/\lambda_0)}{1 + \{\theta_t/(D/D_0)\}k_{s2,0}\lambda_0}\right]$

15. $\log_{10}(D/D_0) = \dfrac{v_f}{A(T) + B(T)v_f}$

16. $v_f = 0.025 + (\alpha_l - \alpha_g)[T - T_g]$

17. $\dfrac{1}{T_g} = \dfrac{1}{T_{g\infty}} + \dfrac{K_s}{T_{g\infty}^2}\dfrac{1}{\bar{\mu}_n}$

[a] Brackets, [ ], for concentrations omitted for brevity.

μ_{n0}, was attained. The rate and equilibrium constants for liquid phase reaction were those reported by Tai et al.[10] as listed in Table II. The results of the liquid phase polymerization as shown in Table VI were found to agree well with values reported previously by Ray and Gupta.[8] The product (quenched) from the liquid phase polymerization was taken as the initial material of the chips undergoing postcondensation. The corresponding initial conditions for SSP at different μ_{n0} are listed in Table VI. Since Gaymans et al.[5] report only the starting values of μ_{n0} for SSP, the other concentrations used by us to simulate their data may be slightly different.

Solid-state polymerization was simulated for a few typical situations, using sets of initial conditions given in Table VI, by solving the set of partial differential equations in Table V. It was assumed, earlier, that the four intrinsic rate constants, $k_{s2,0}$, $k_{s3,0}$, $k'_{s2,0}$, and $k'_{s3,0}$, were given by the expressions of Tai et al.[10] (Table II). It was observed that this choice of intrinsic rate constants led to a very slow increase in the number-average chain length with time, as compared with the experimental data of Gaymans et al.[5] Indeed, one should not expect the rate constants of Tai et al. to be valid at temperatures below the melting points since they were obtained from experimental data on liquid phase polymerization. We, therefore, considered the intrinsic rate constants as follows:

$$k_{s2,0} = \zeta_2(T)\lambda_0 \tag{24a}$$

$$k_{s3,0} = \zeta_3(T)\lambda_0 \tag{24b}$$

with $\zeta_2(T)$ and $\zeta_3(T)$ as parameters. The catalytic effect of the acid end groups, as found for the liquid phase polymerizations, has been assumed to be valid for solid phase as well and is reflected by the presence of λ_0 in Eq. (24). Assuming that the values of the equilibrium constants, K_2 and K_3, reported by Tai et al. for liquid phase polymerization are valid for the polymerization in the solid phase as well, values of the intrinsic reverse rate constants are obtained by

$$k'_{s2,0} = \frac{k_{s2,0}}{K_2} \tag{25a}$$

$$k'_{s3,0} = \frac{k_{s3,0}}{K_3} \tag{25b}$$

These equations, as well as the model for k_{s2}, are also included in Table V. Thus, Table V gives the complete set of equations required to simulate the SSP of nylon 6.

The reference values of the various parameters and the polymerization conditions used in Table V are listed in Table VII. The values of $A(T)$ and $B(T)$ used at 473.16 K are those used by Kumar et al.[4] The value of $T_{g\infty}$ has been taken from Ref. 11. $K_s/T_{g\infty}^2$ has been chosen so that Eq. (18) predicts a glass transition temperature of about 320–330 K at a number-average chain length of about 140–160.

Table VI Starting Concentrations for Solid Phase Reaction[a]

Species	Concentrations Corresponding to Different μ_{n0}				
	$\mu_{n0} = 22$	35	55	72	95
C_1	8.106	7.267	5.869	4.842	3.660
P_1	0.00075	0.00068	0.0006	0.00055	0.00049
λ_0	0.03122	0.04331	0.05244	0.05456	0.05367
λ_1	0.69388	1.53307	2.93076	3.95800	5.13901
λ_2	22.10	80.43	260.10	485.20	902.20
W	0.10510	0.08763	0.09683	0.0949	0.0957

[a] Initial conditions in liquid phase polymerization to obtain the above values:

Temperature = 513.0 K
$C_{1,0}$ = 8.80 mol/kg
$P_{1,0}$ = 0.0 mol/kg
$\lambda_{0,0}$ = 0.0 mol/kg
$\lambda_{1,0}$ = 0.0 mol/kg
$\lambda_{2,0}$ = 0.0 mol/kg
W_0 = 0.16 mol/kg

For selecting this range of glass transition temperature and the corresponding range of the chain length, we were guided by several papers published on glass transitions and mechanical relaxations in polyamides.[12-21] It should be emphasized here that these parameters (A, B, $T_{g\infty}$ and $K_s/T_{g\infty}^2$) can be found by independent measurements even on nonreacting systems. The reference value of θ_t (1000 h) has been so selected as to give a reasonable decrease in $k_{s2}/k_{s2,0}$ as the reaction proceeds. The reference values of ζ_2 and ζ_3 have been chosen such as to give

Table VII Reference Value of Parameters and Conditions Used for Simulation

Parameters

θ_t = 1000 h
ζ_2(463.16 K) = 200 kg^2/mol^2 h
ζ_3(463.16 K) = 40 kg^2/mol^2 h

Other Parameters and Conditions

A(463.16 K) = 0.04
B(463.16 K) = 0.03
$T_{g\infty}$ = 350 K
$\frac{K_g}{T_{g\infty}^2}$ = 0.03 K^{-1}
$D_w = 10^{-11}$ m^2/h
$\alpha_l = 10^{-3}$ K^{-1}
$\alpha_g = 4.5 \times 10^{-4}$/K
T = 463.16 K
$R = 2 \times 10^{-4}$ m
$[W]_s$ = 0.0001 mol/kg

simulation results that approximated the experimental data reported by Gaymans et al.[5] θ_t, ζ_2, and ζ_3 are, thus, the three curve-fit parameters in this model. The value of $[W]_s$ has been chosen somewhat arbitrarily for the present analysis since it is not reported by Gaymans et al.[5] $[W]_s$ is selected as a very low value compared to the concentration of water inside the reacting pellet. Since the results are found to be relatively insensitive to $[W]_s$ around this value, this assumption does not introduce any error. The values of the coefficients of thermal expansion for liquid and glassy polymers, α_l and α_g, respectively, listed in Table VII, have been obtained from the literature.[11]

Even though the parameters, $A(T)$, $B(T)$, and $K_s/T_{g\infty}^2$, can be actually obtained from independent measurements, they have been included along with θ_t, ζ_2, and ζ_3 in an optimal parameter estimation program to obtain best-fit values for them using the experimental isothermal data on nylon 6. A Box-complex algorithm[23] has been used for this purpose. The objective function that has been minimized in this program is given by

$$F(x) = \text{Max}\left[-\sum_{j=1}^{N} \frac{|\mu_{n,\text{expt}}(j) - \mu_{n,\text{theor}}(j)|}{\mu_{n,\text{theor}}(j)}\right] \quad (26)$$

where N is the total number of experimental data points for all μ_{n0} reported. The best-fit values of the parameters so obtained are given in Table VIII. It is interesting to note that the optimal values of B (463.16 K) and $K_s/T_{g\infty}^2$ come out to be identical to the reference values in Table VII.

Table VIII Optimum Values of Parameters

θ_t	= 1000 h
ζ_2(463.16 K)	= 200 kg^2/mol^2 h
ζ_3(463.16 K)	= 40 kg^2/mol^2 h
A(463.16 K)	= 0.03
B(463.16 K)	= 0.03
$K_s/T_{g\infty}^2$	= 0.03 K^{-1}

RESULTS AND DISCUSSION

Figures 2–6 show simulation results for the spatial average value of the number-average chain length, $\bar{\mu}_n$ vs. time, for five different values of μ_{n0}, using the optimal values for the various parameters (Table VIII). Experimental data points as well as the smoothed experimental curves have also been shown in these diagrams for comparison. The simulation results are found to be in reasonable agreement with the experimental data, specially if we remember that the precise starting values of $[C_1]$, $[W]$, λ_0, and λ_1 used by Gaymans et al.[5] in their experiments have not been reported. It is observed that the higher the value of μ_{n0}, the faster is the rate of reaction, and consequently, the higher is the mean number-average chain length at the end of the reaction. Figures 2–6 indicate that the model results fit experimental data better when μ_{n0} is larger than about 22 (note that the data point at t = 24 h in Fig. 6 is a lone point, the earlier point being at t = 8 h, and so we do not give it too much importance). A likely cause for the discrepancy at low μ_{n0} could be the importance of the ring-opening reaction (see Table I) in these cases, which has been neglected in our model for SSP. Also, it is expected that the initial value of

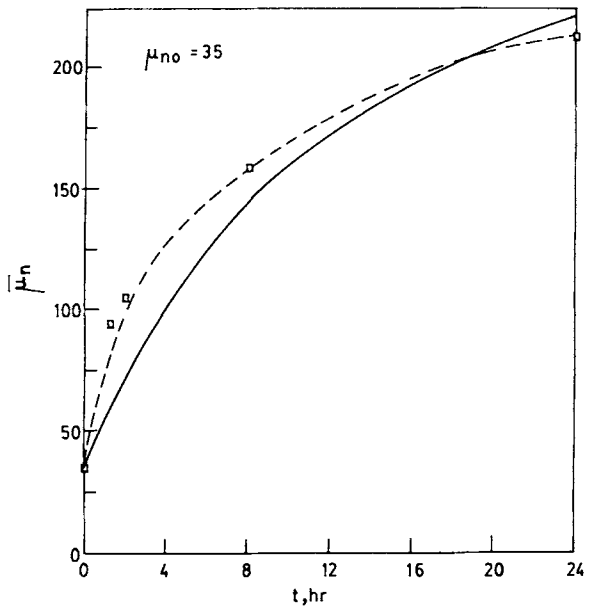

Figure 3 Comparison of experimental (– – –) and simulation (——) results, μ_{n0} = 35.

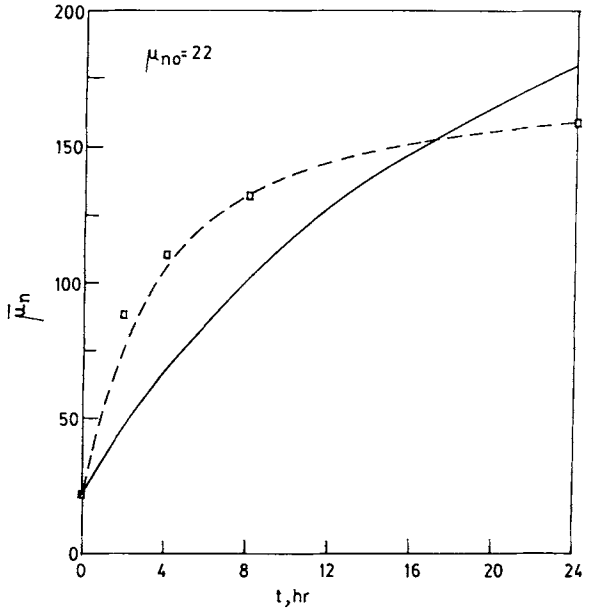

Figure 2 Comparison of experimental (– – –) and simulation (——) results, μ_{n0} = 22.

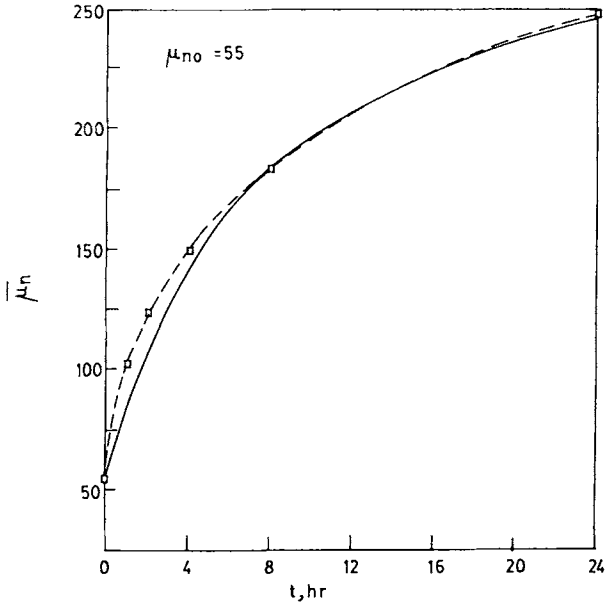

Figure 4 Comparison of experimental (– – –) and simulation (——) results, μ_{n0} = 55.

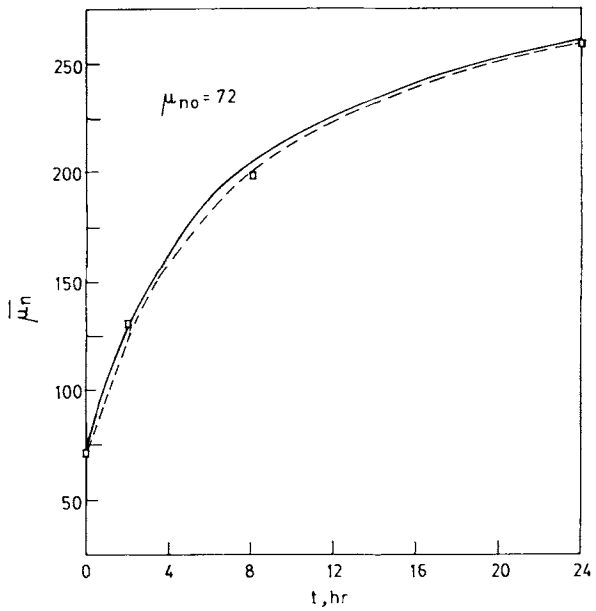

Figure 5 Comparison of experimental (- - -) and simulation (——) results, $\mu_{n0} = 72$.

$[C_1]$, $[W]$, and the moments would play a more crucial role in the low μ_{n0} runs than in higher μ_{n0} cases, and the lack of precise experimental values for these could also be partly responsible for the discrepancy.

It is interesting to note that the optimal values (Table VIII) obtained by curve fitting experimental data are quite close to the reference values, for those parameters that have been obtained from the literature based on independent measurements. In fact, one could easily have fixed the values of A, B, $T_{g\infty}$, and $K_s/T_{g\infty}^2$ at their literature values and obtained optimal curve-fit values for the three parameters, θ_t, ζ_2, and ζ_3. Thus, our optimal parameter estimation is quite justified.

The effect of varying each of the parameters, A, B, θ_t, $K_s/T_{g\infty}^2$, ζ_2, and ζ_3, one by one around the optimal values shown in Table VIII, is shown in Figures 7–12. The value of μ_{n0} used in these is 72. Figures 7 and 8 show the effect of the parameters $A(T = 463.16\ \text{K})$ and $B(T = 463.16\ \text{K})$ on the progress of the reaction. These plots indicate that increasing either A or B slows down the progress of reaction, though the effect of A is more drastic. It is also observed from Figure 7 that the effect of A is more pronounced at higher chain lengths than at lower values. This is because at higher chain lengths the free volume fraction of the reacting mass is small, and under these conditions $A(T)$ plays a more important role in determining the value of D/D_0 in Eq. (15). The sensitivity of the results to A in the range 0.04–0.07 should be noted.

The effect of the characteristic migration time, θ_t, on the number-average chain length is shown in Figure 9. The plot shows that for θ_t varying from about 0–100 h, the effect is almost insignificant. As the value of θ_t is increased from about 100 to 5000

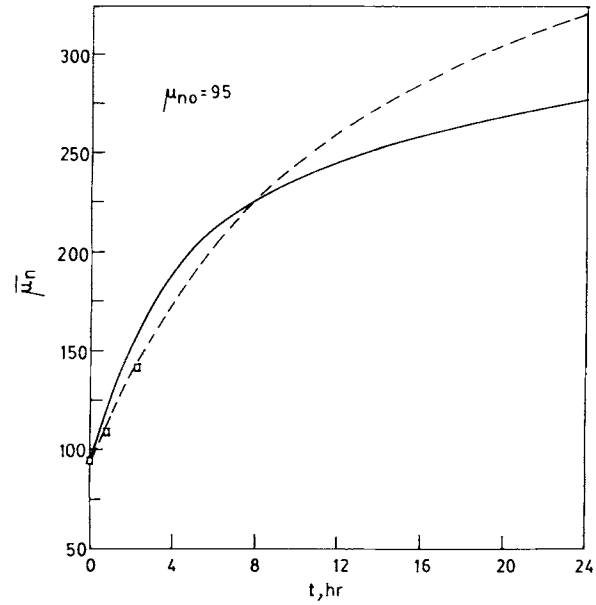

Figure 6 Comparison of experimental (- - -) and simulation (——) results, $\mu_{n0} = 95$.

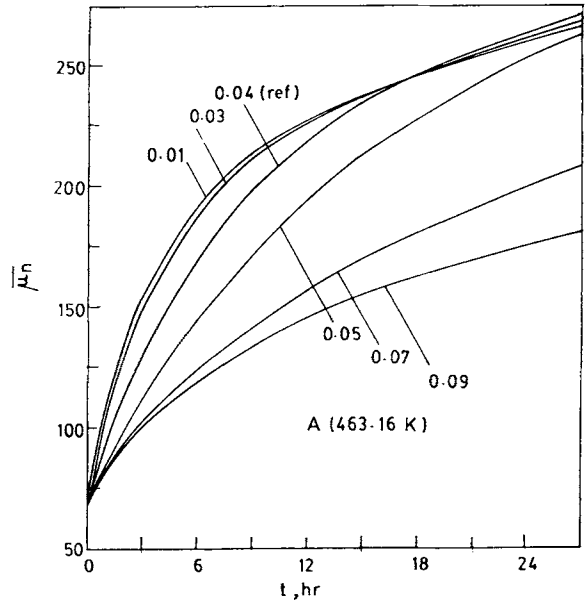

Figure 7 Effect of the parameter $A(T = 463.16\ \text{K})$ on $\bar{\mu}_n$; $\mu_{n0} = 72$.

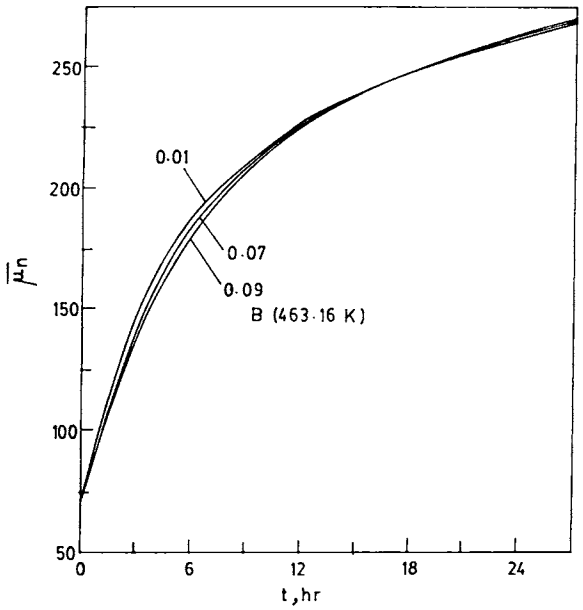

Figure 8 Effect of the parameter $B(T = 463.16\ \text{K})$ on $\bar{\mu}_n$; $\mu_{n0} = 72$. Reference value of B is 0.03.

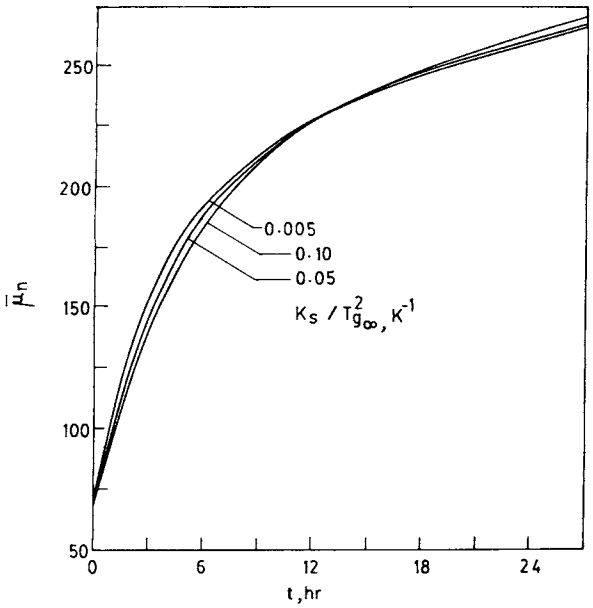

Figure 10 Effect of $K_s/T^2_{g\infty}$ on $\bar{\mu}_n$; $\mu_{n0} = 72$. Reference value of $K_s/T^2_{g\infty}$ is 0.03.

h, the progress of reaction is affected significantly. At a value of θ_t above 10,000 h the effect on the progress of reaction is relatively insignificant. Figure 10 gives the plot of $\bar{\mu}_n$ vs time for various values of the parameter $K_s/T^2_{g\infty}$. This parameter determines how the glass transition temperature, T_g, varies with the chain length, and the value of T_g directly affects the free volume fraction of the reacting mass, and so the effective diffusivity. Figure 10 indicates, however, that the number-average chain length of the polymer remains almost unaltered with time as the value of $K_s/T^2_{g\infty}$ is varied from about 0.005 to 0.1 K^{-1}. Figures 11 and 12 show the effect of the parameters $\zeta_2(T = 463.16\ \text{K})$ and $\zeta_3(T = 463.16\ \text{K})$ on the number-average chain length. It is interesting to note that as the value of ζ_2 is varied from 10 to

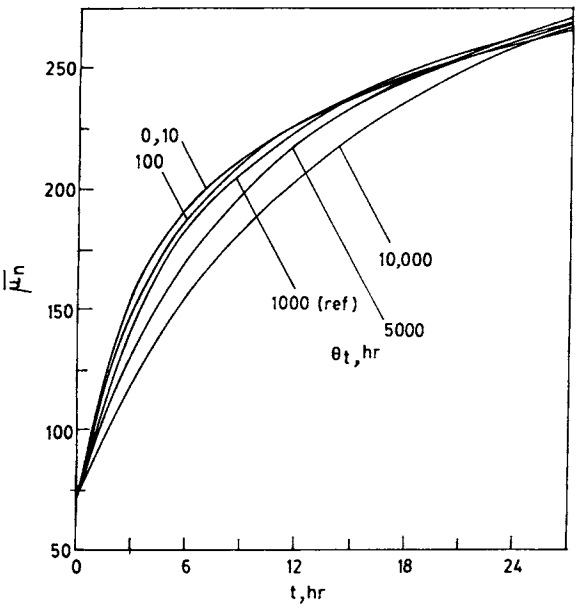

Figure 9 Effect of the parameter, θ_t, on $\bar{\mu}_n$; $\mu_{n0} = 72$.

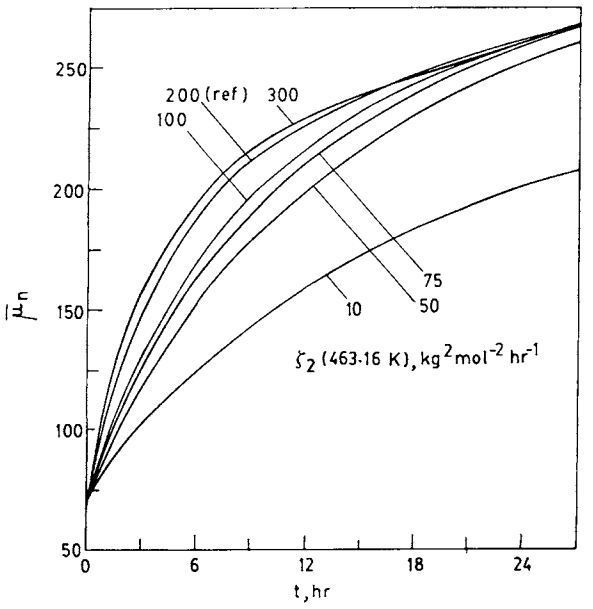

Figure 11 Effect of the parameter $\zeta_2(T = 463.16\ \text{K})$ on $\bar{\mu}_n$; $\mu_{n0} = 72$.

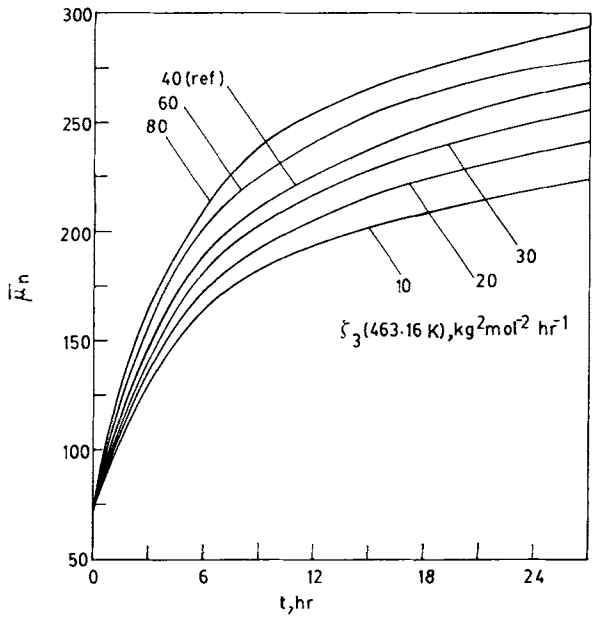

Figure 12 Effect of the parameter $\zeta_3(T = 463.16\ \text{K})$ on $\bar{\mu}_n$; $\mu_{n0} = 72$.

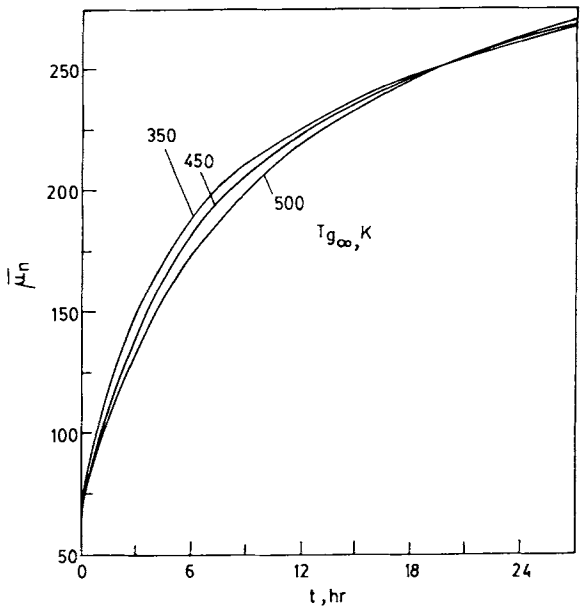

Figure 13 Effect of $T_{g\infty}$ (K) on the mean number-average chain length of nylon 6 undergoing SSP, $\mu_{n0} = 72$. Reference value of $T_{g\infty}$ is 350 K.

200 kg^2/mol^2 h, the value of the forward rate constant for the polycondensation reaction varies from 0.5 to 10 kg/mol h [for $\lambda_0 \cong 0.05$ mol/kg]. The corresponding value of the rate constant (at $T = 463.16$ K) using the correlation of Tai et al.[10] (for liquid phase polymerization, see Table II) is about 0.275 kg/mol h. The rate constants for SSP are, thus, observed to be almost an order of magnitude higher than values predicted at the same temperature by Tai et al. for polycondensation in the liquid phase. Figure 11 indicates that as the value of the parameter, ζ_2, characterizing the forward rate constant, k_{s2}, is increased the progress of reaction is faster. This is to be expected. The most drastic effect is observed when ζ_2 varies from about 10 to 50 kg^2/mol^2 h. The effect of ζ_2 above a value of about 200 kg^2/mol^2 h becomes relatively insignificant. The effect of ζ_3 is more gradual as compared to that of ζ_2. The variation in ζ_3 from 10 to 80 kg^2/mol^2 h, gives a corresponding variation in the value of the forward rate constant of the polyaddition reaction from about 0.5 to 4 kg/mol h [for $\lambda_0 \cong 0.05$ mol/kg]. The corresponding value of the rate constant for this reaction given by the correlations of Tai et al. (Table II) is about 0.27 kg/mol h. Once again, the higher values of the rate constants associated with SSP are to be noted. The progress of reaction is observed to be enhanced as the value of ζ_3 is increased.

The effect of varying some other parameters and conditions has also been studied. It has been found that the increase in $\bar{\mu}_n$ with time is unrealistically high when the value of the (macro)diffusivity of water, D_w, is larger than about 10^{-10} m^2/h. However, $\bar{\mu}_n$ varies significantly with time when the value of D_w is changed between 10^{-10} and 10^{-12} m^2/h, and

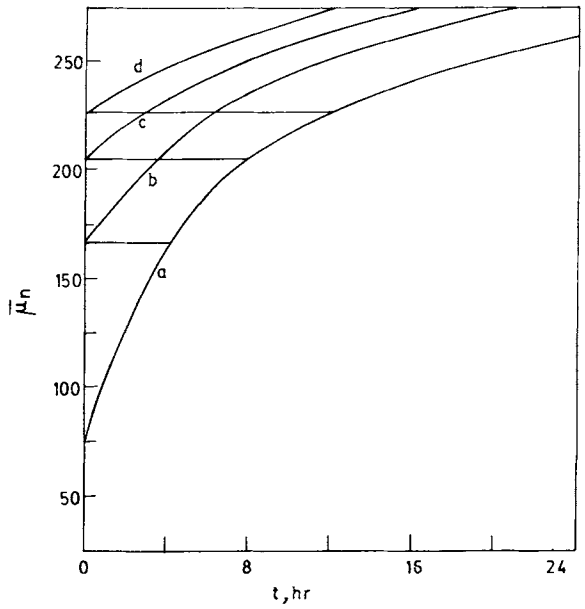

Figure 14 Comparison of the results for SSP after remelting the polymer sample after (b) 4, (c) 8, and (d) 12 h of SSP, with (a) no remelting of polymer, $\mu_{n0} = 72$.

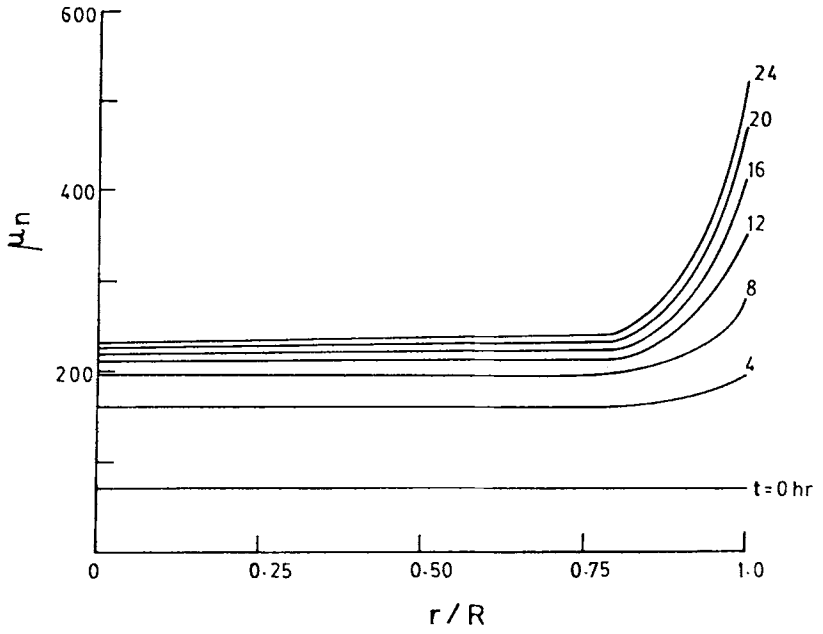

Figure 15 Radial profiles for μ_n at different times, $\mu_{n0} = 72$.

remains essentially constant for values of D_w below about 10^{-13} m^2/h. When the surface water concentration, $[W]_s$, is changed almost a thousand fold from 0.0001 to 0.1 mol/kg, it is found that the increase in the mean value of the number-average chain length, $\bar{\mu}_n$, is insensitive to changes in $[W]_s$. A similar observation is made when the pellet radius is varied from 2×10^{-4} to 1.6×10^{-3} m. There is some doubt about the value of $T_{g\infty}$ for nylon 6. Figure 13 shows the effect of varying $T_{g\infty}$. Higher values of $T_{g\infty}$ are found to suppress the rate of solid-state polymerization of nylon 6, though not very significantly. Some results were also generated with slightly different values of equilibrium constants (at 463.16 K), than given by Tai et al. (Table II). It was found that the results were relatively insensitive to variations in K_3. Also, the values of $\bar{\mu}_n$ were found to depend on the value of K_2 used, but only after a polymerization time of about 12 h.

Figure 14 shows what happens when a polymer sample with $\mu_{n0} = 72$ is remelted (homogenized) and then subjected to further polymerization in the solid phase. The plot indicates that there is an increase in the rate of polymerization if the polymer sample is remelted after some time. This trend is *qualitatively* similar to the experimental observations of Gaymans et al.[5] (who do not provide sufficient experimental details for us to attempt a quantitative comparison) and thus lends support to the molecular mechanism underlying the phenomenon of SSP.

We also studied the variation of μ_n and $[W]$ with radial location (Figures 15 and 16, respectively). It was observed that at any time, μ_n was almost uniform along the position, except for the outer 20% of the sphere, where μ_n went up significantly. In this region $[W]$ was found to decrease. Figures 15 and 16 show the profiles for conditions given in Table VIII. We

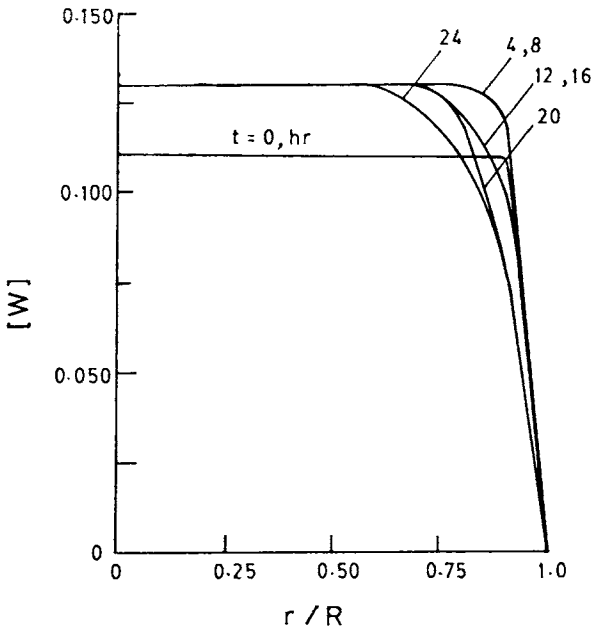

Figure 16 Radial profiles for $[W]$ at different times, $D_w = 10^{-11}$ m^2/h, $\mu_{n0} = 72$.

believe that using the local value of μ_n in Eq. (18) instead of the spatial average value, $\bar{\mu}_n$, will not lead to significant error in view of the fact that only a small region exists where μ_n is high, and the effect of μ_n on $\bar{\mu}_n(t)$ would be similar to that of $K_s/T_{g\infty}^2$ [see Eq. (18) and Fig. 10].

CONCLUSIONS

A model having a strong molecular basis for the SSP of nylon 6 has been proposed in this work. It is observed that using essentially three parameters, θ_t, ζ_2, and ζ_3, one can explain some limited experimental data on nylon 6 quite well. The model also predicts the qualitative trends observed experimentally on the SSP of nylon 6 chips with intermediate remelting. It is found that the rate constants are higher for SSP than predicted by the correlations of Tai et al.,[10] which have been obtained for the melt polymerization of nylon 6. More and comprehensive experimental data on the SSP of nylon 6 is required to obtain the three parameters at different temperatures. The present model, because of its more fundamental basis than earlier models on SSP, offers a better basis for the scale-up of industrial SSP reactors.

NOMENCLATURE

A_i^0 Arrhenius frequency factor for ith uncatalyzed reaction in liquid phase, kg/mol h.

A_i^c Arrhenius frequency factor for ith catalyzed reaction in liquid phase, kg^2/mol^2 h.

—A Polymer molecule with an unreacted A group.

$A(T)$ Parameter in free volume equation.

—B Polymer molecule with an unreacted B group.

$B(T)$ Parameter in free volume equation.

C_1 ϵ-Caprolactam.

D Overall (micro) diffusivity of polymer molecule, m^2/h.

D_0 Overall diffusivity of polymer molecule at some reference condition, m^2/h.

D_w Diffusivity (macro) of water inside the reacting pellet, m^2/h.

E_i^0 Activation energy for ith uncatalyzed reaction in liquid phase, J/mol.

E_i^c Activation energy for ith catalyzed reaction in liquid phase, J/mol.

ΔH_i Change in enthalpy of ith reaction in liquid phase, J/mol.

k_{li} Forward rate constant of ith reaction in liquid phase, kg/mol h.

k'_{li} Reverse rate constant of ith reaction in liquid phase, kg/mol h.

k_{si} Overall forward rate constant of ith reaction in the solid phase, kg/mol h.

k'_{si} Overall reverse rate constant of ith reaction in the solid phase, kg/mol h.

$k_{si,0}$ Intrinsic forward rate constant of ith reaction in the solid phase, kg/mol h.

$k'_{si,0}$ Intrinsic reverse rate constant for ith reaction in the solid phase, kg/mol h.

k_p Overall forward rate constant for ARB polymerization, kg/mol h.

k'_p Overall reverse rate constant for ARB polymerization, kg/mol h.

k_{p0} Intrinsic forward rate constant for ARB polymerization, kg/mol h.

k'_{p0} Intrinsic reverse rate constant for ARB polymerization, kg/mol h.

K_i Equilibrium constant of ith reaction.

K_s Parameter in equation for glass transition temperature, K.

P_n Polymer molecule of chain length n.

$[P]_m$ Concentration of polymer molecule P at radius r, mol/kg.

$[P]_b$ Bulk concentration of polymer molecule P, mol/kg.

r_m Radius swept by a polymer molecule having one unreacted A group fixed at one end, m.

r_D Radius at which the concentration of polymer molecule P approaches the bulk value, m.

R Radius of the solid pellet, m; also, Gas constant in Table II, J/mol K.

ΔS_i Change in entropy for ith reaction in the liquid phase, J/mol K.

T Reaction temperature, K.

T_g Glass transition temperature, K.

$T_{g\infty}$ Glass transition temperature at infinite chain length, K.

v_f Free volume fraction inside the reacting pellet.

$[W]_s$ Surface concentration of water, mol/kg.

Greek Letters

α_l Coefficient of thermal expansion of polymer in liquid state, K^{-1}.

α_g Coefficient of thermal expansion of polymer in glassy state, K^{-1}.

ζ_j Parameter used in the forward rate constant for jth reaction in solid phase, kg^2/mol^2 h.

λ_k kth moment of all polymer molecules, $\lambda_k = \sum_{n=1}^{\infty} n^k[P_n]$, mol/kg.

λ_{1b} Bulk value of the first moment, mol/kg.

θ_t Parameter denoting characteristic time of migration, h.

μ_n Number-average chain length = λ_1/λ_0.

$\bar{\mu}_n$ Spatial average value of $\mu_n = (\int_0^R r^2\lambda_0\, dr)/(\int_0^R r^2\lambda_0\, dr)$

REFERENCES

1. F. Pilati, in *Comprehensive Polymer Science,* Vol. 5, *Step Polymerization;* G. C. Eastmond, A. Ledwith, S. Russo, and P. Sigwalt, Eds., Pergamon, New York, 1989, pp. 201.
2. F. C. Chen, R. G. Griskey, and G. H. Beyer, *AIChEJ,* **15,** 680 (1969).
3. W. Y. Chiu, G. M. Carratt, and D. S. Soong, *Macromolecules,* **16,** 348 (1983).
4. A. Kumar, K. Saxena, J. P. Foryt, and S. K. Gupta, *Polym. Eng. Sci.,* **27,** 753 (1987).
5. R. J. Gaymans, J. Amritharaj, and H. Kamp, *J. Appl. Polym. Sci.,* **27,** 2513 (1982).
6. R. G. Griskey and B. I. Lee, *J. Appl. Polym. Sci.,* **10,** 105 (1966).
7. A. Ramgopal, A. Kumar, and S. K. Gupta, *J. Appl. Polym. Sci.,* **28,** 2261 (1983).
8. A. K. Ray and S. K. Gupta, *J. Appl. Polym. Sci.,* **30,** 4529 (1985).
9. G. B. McKenna, in *Comprehensive Polymer. Science* Vol. 2, *Polymer Properties,* C. Booth, and C. Price, Eds., Pergamon, New York, 1989, pp. 311.
10. K. Tai and T. Tagawa, *Ind. Eng. Chem., Prod. R&D,* **22,** 192 (1983).
11. D. W. Van Krevelen, *Properties of Polymers,* 2nd ed., Elsevier, New York, 1974.
12. R. F. Boyer, in *The Solid State of Polymers: Report of the US-Japan Joint Seminar,* P. H. Geil, E. Baer, and Y. Wada, Eds., Marcel Dekker, New York, 1974, p. 503.
13. L. E. Nielsen, *Mechanical Properties of Polymers and Composites,* Vol. 1, Marcel Dekker, New York, 1974.
14. J. Brandrup and E. H. Immergut, *Polymer Handbook,* 2nd ed., Wiley-Interscience, New York, 1975.
15. D. C. Prevorsek, R. H. Butler, and H. K. Reimschuessel, *J. Polym. Sci. A2,* **9,** 867 (1971).
16. G. A. Gordon, *J. Polym. Sci. A2,* **9,** 1693 (1971).
17. J. Kolarik and J. Janacek, *J. Polym. Sci. C1,* **16,** 441 (1967).
18. A. Anton, *J. Appl. Polym. Sci.,* **12,** 2117 (1968).
19. F. Rybnikar, *J. Polym. Sci.,* **28,** 633 (1958).
20. T. Shibusawa, *J. Appl. Polym. Sci.,* **14,** 1553 (1970).
21. F. R. Prince, E. M. Pearce, and R. J. Fredericks, *J. Polym. Sci. A1,* **8,** 3533 (1970).
22. V. Frosini and E. Butta, *J. Polym. Sci. B,* **9,** 253 (1971).
23. J. L. Kuester and J. H. Mize, *Optimization Techniques with Fortran,* 1st ed., McGraw-Hill, New York, 1973.

Received May 3, 1991
Accepted August 1, 1991